IOP Conf. Series: Materials Science and Engineering **241** (2017) 012014 doi:10.1088/1757-899X/241/1/012014

Research on wire rope stress distribution of WR-CVT

Wu Zhang, Wei Guo, Chuanwei Zhang, Zhengxiong Lu, Xiaobin Xu

School of Mechanical Engineering, Xi'an University of Science and Technology, Xi'an, Shaanxi , 710054, China

corresponding author's: zhangwu0828@163.com

Abstract. A wire rope continuously variable transmissions (WR-CVT) has been introduced in the paper, in view of its less research, this paper mainly studied the stress distribution of 6×7+IWS bending wire rope. The results shown that the wire stress is layered distribution in each section, the stress at the outer strand center wire and outer strand side wire was the greatest, the stress value of the outer strand side wire and metal block circular notch is second. As the transmission ratio decreases, the wire stress decreases, which is related to the pulley working radius increases. Compared with the section A1, the stress value on the section A2 is smaller, mainly because the section A2 is not in contact with the metal block or the contact pressure is small. This study provides a basis for the study of fatigue and wears failure of WR-CVT components.

1. Introduction

Over the past two decades, continuously variable transmissions (CVT) have aroused a great deal of interest in the automotive sector due to the potential of lower emissions and better performance [1]. Metal pushing V-belt and metal chain CVT have been developed for automotive applications. In a comparison of the fuel consumptions of vehicles with different transmission types on the US market for the US Environmental Protection Agency city cycle [2], it was seen that, generally, vehicles with CVT achieve a higher fuel economy than vehicles with stepped automatic trans-missions do. According to forecasts made by CSM Worldwide [3], it is expected that the market share of CVT equipped vehicles will keep growing in the future. Nowadays CVT are widely used in agricultural vehicles, mini cars and motor-cycles, and more and more attention is placed on vehicle com-fort, fuel economy and low environmental impact. To achieve this objective, a continuously variable transmission could be helpful [4]. Wang, Dagang, et al [5] researched the stress distributions along the contact path (between the rope and friction lining) by using finite element analyses, the result indicate that with an increases of hoisting parameters, the stress concentrations increases. A wire rope CVT (WR-CVT) has been designed by Wu Zhang et al [6], WR-CVT as shown in Figure 1. Traditional wire ropes are commonly used in long-distance and low-speed transmission systems, and the CVT is classed as a high-speed transmission system. Therefore, the application of closed wire rope not only enhances the CVT-product type, but also extends the application of closed wire ropes. The knit method and the manufacturing level of this closed wire rope place higher demands, requiring advanced technologies to be developed. WR-CVT requires suited to the passenger cars and motorcycles.

2 Closed wire rope geometry model

In this paper, the wire rope model is 6×7+IWS. It contains 1 core strand and 6 side strands, one strand

contains a center wire and six side wires. 6×7+IWS contains four different geometric forms of wire, they are core strand center wire, core strand side wire, outer strand center wire and outer strand side wire. Core strand center wire is the axis of closed wire rope, core strand side wire and outer strand center wire are single helix, Outer strand side wire is second helix. 6×7+IWS wire rope section is shown in **Figure. 2.**

According to the right-hand rules to establish a Cartesian coordinate system O-xyz as a closed wire rope mathematical model of the global coordinate system[7,8], the centerline equation for each wire in a closed wire rope is given [9,10], Wire rope specific parameters References [11]. The 3D solid model of 6×7+IWS bending wire rope was established by using parametric modeling and surface modeling of Pro/E, as shown in **Figur**e.3.

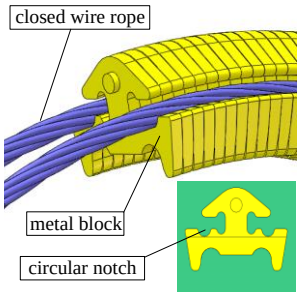

Fig. 1. WR-CVT

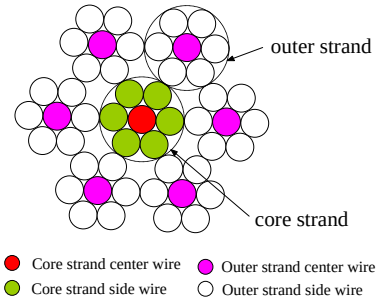

Fig. 2. 6×7+IWS wire rope section

Fig.3 6×7+IWS 3D solid model

3 Wire rope mesh generation and Section definition

3.1 Wire rope mesh generation

The selection of the wire rope length is very important for the finite element analysis. Wire rope is too short can not fully contact between the wire rope and too long will affect the calculation efficiency. In order to obtain higher analytical precision and computational efficiency, we select one-twist length steel rope loop as the analysis model in this paper. The ABAQUS software was used for the finite element modeling. The wire material model is defined by the following parameters: Modulus of elasticity E= 1.96×10^{11}Pa, Yield limit: σ_s=1.54×10^{9}Pa, Shear modulus G=8.53×10^{10}Pa, Poisson ratio μ=0.3, Friction coefficient f=0.115. Definition of closed wire rope and metal block unit property type C3D8R hexahedron. According to the calculation requirements, select the appropriate grid size, complete the meshing in Hypermesh, the number of divisions is 67982, the number of nodes is 94994, as shown in Figure 4. In the finite element model of the wire rope, one end applies the surface constraint, restrains all degrees of freedom in three directions, *x*, *y*, *z*, and applies the surface load at the other end.

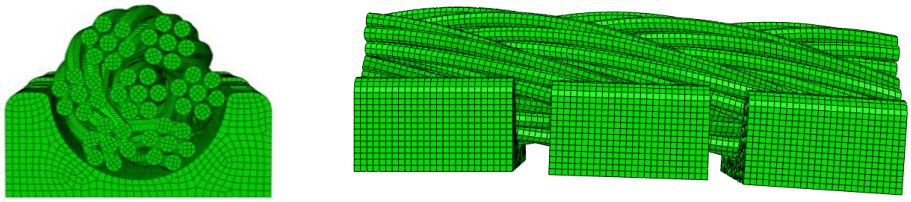

Fig.4 Wire rope mesh generation

3.2 Section definition

When the transmission ratio i=0.42, the angle between the two cross sections is 1.6 ° and 2.6 °, respectively, and is defined as the section A_1 and the section A_2. The following main analysis of the two sections of the steel wire stress distribution. Figure 5 is the section position; Figure 6 is the wire number and path schematic.

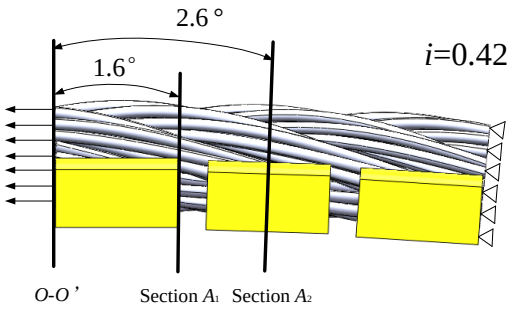

Fig.5 Section position

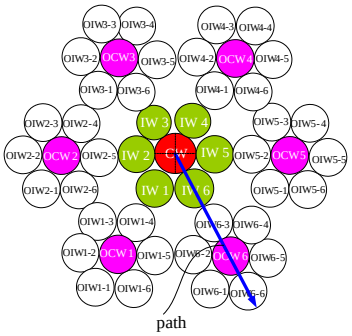

Fig.6 Wire number and path schematic

4 Wire rope stress analysis

Figure 7 shows the transmission ratio *i*=0.42, the driving pulley bending section of the overall stress distribution of the rope ring. It can be seen from the figure 7: the wire stress along the direction of rotation of the wire rope staggered distribution.

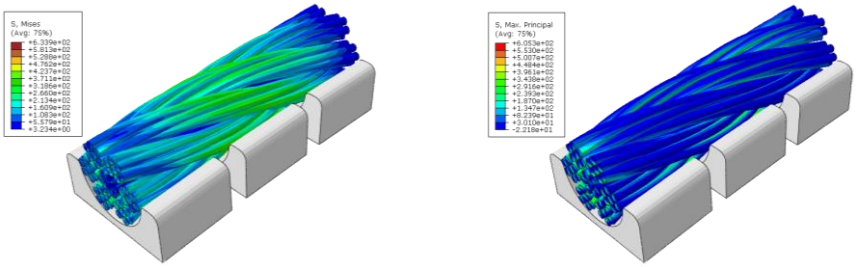

(*a*) Equivalent stress (*b*) The maximum stress

Fig.7 Wire rope stress distribution (*i*=0.42)

Figure 8 is the wire maximum stress distribution of section A_1 and A_2 in. It can be seen from the figure that the stress distribution of the steel wire is symmetrical in the left and right, and asymmetrical in the up and down direction. The wire stress on the side of the metal block circular notch is less than that on the other side. The stress in each section of the wire is in the form of a layer distribution, the middle stress is small, and the stress on the contact side with other steel wires is larger. In section A_1, the maximum stress value is located in the wire contact with the edge of the metal block circular notch, and the stress value is much higher than other wire, indicating that the two wire stress concentration is the most serious, and thus more prone to early failure. In Section A_2, although the value of the stress of the wire near the side of the rope circular notch is high, the stress difference of each wire is small and the distribution is relatively uniform.

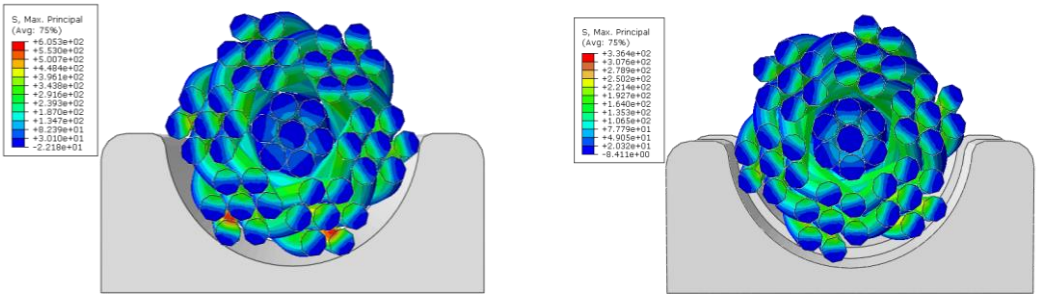

(*a*) The maximum stress of section A_1 (*b*) The maximum stress of section A_2

Fig.8 wire stress (*i*=0.42)

When the transmission ratio for other values, the stress profile on each section is similar to Figure 8, here is no longer shown, only the value extracted.

Figure 9 shows the wire stress distribution along the path in sections A_1 and A_1 for transmission ratios *i*=2.35, 1.0 and 0.42. Figure 9 (*a*) shows that with the decrease of the transmission ratio, the wire stress is decreasing. Among them, the core strand side wire in the different transmission ratio stress is

basically the same. The lateral stress of the outer strands was the highest, and the maximum value of the stress appeared at the contact point between the outer strand center wire and the outer strand side wire because of the influence of the metal block circular notch. The wire stress at the corresponding position decreases as the transmission ratio decreases.

Figure 9 (*b*) shows that as the transmission ratio decreases, the overall stress of steel wire are still decreasing. The stress difference of the upper side steel wire is smaller and the stress distribution is more uniform. The stress of the side wire in contact with the metal block circular notch is larger, and the maximum value is in contact with the center filament of the side strands, which is similar to the section A_1.

Since the section A_2 is not in contact with the metal block or the contact pressure is small, the stress value on the section A_2 is generally smaller in comparison with the section A_1.

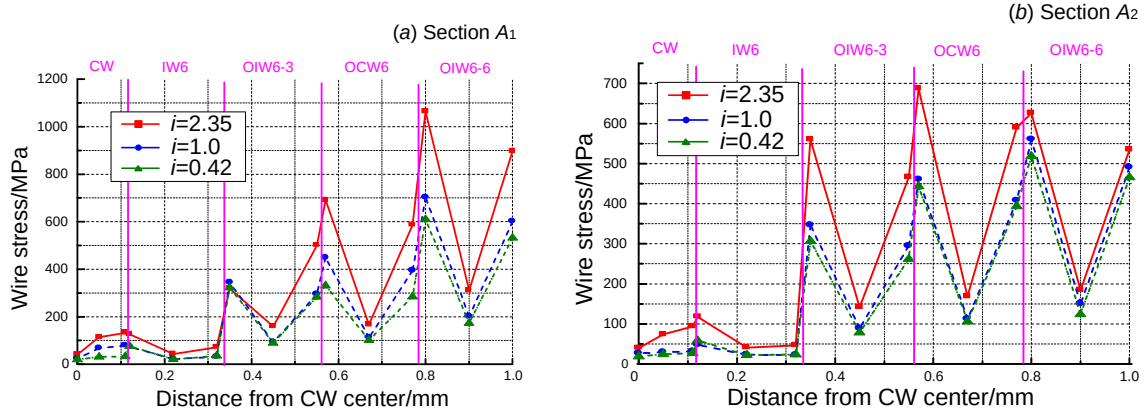

Fig.9 Stress distribution of wire along path

5. Conclusion

In this paper, the stress distribution of WR-CVT bending wire rope is mainly studied. The geometrical model of 6×7+IWS bending wire rope is established by Pro/E software. The finite element model of bending wire rope is completed by ABAQUS software. The stress distribution of the wires on the two sections is analyzed. The results shown that the stress in each section of the wire is in the form of layered distribution, the middle stress is small, and the stress in contact with other wires is larger. The stress at the outer strand center wire and outer strand side wire was the greatest, the stress value of the outer strand side wire and metal block circular notch is second. As the transmission ratio decreases, the wire stress decreases, which is related to the pulley working radius increases. Compared with the section A_1, the stress value on the section A_2 is smaller, mainly because the section A_2 is not in contact with the metal block or the contact pressure is small.

Acknowledgement

The research presented here was supported by the National Natural Science Foundation of China (Grant No.51505373). The authors are grateful for the support.

References

[1] Nilabh Srivastava, Imtiaz Haque. Clearance and friction-induced dynamics of chain CVT drives[J]. *Multibody System Dynamics*, 2008, 19(3): 255-280

[2] FVD Sluis, AVD Velde, TV Dongen, GJV Spijk, AV Heeswijk. Efficiency optimization of the push belt CVT, *SAE paper* 2007-01-1457, 2007.

[3] Doi T. New compact, lightweight, low friction CVT with wide ratio coverage[C]. 2010 international continuously variable and hybrid transmission congress, Maastricht, The Netherlands, 17–19 November 2010. Eindhoven: Eindhoven University of Technology: 146–151.

[4] G. Carbone, L. Mangialardi, G. Mantriota. Influence of clearance between plates in metal pushing V-Belt dynamics[J]. *Journal of Mechanical Design*, 2002, 124(9): 543-557

[5] Wang, Dagang; Li, Xiaowu; Wang, Xiangru; Shi, Ganyu; Mao, Xianbiao; Wang, Dao'Ai. Effects of

hoisting parameters on dynamic contact characteristics between the rope and friction lining in a deep coal mine[J]. *Tribology International*, 2016, 96(4): 31-42.

[6] Zhang Wu, Guo Wei, Lu Zhengxiong, Cao Jianbo. Design and Analysis of a New Metal Belt Continuously Variable Transmission[J]. *Journal of Mechanical Transmission*, 2015, 39(9): 59-61, 88

[7] Lee W K. An insight into wire rope geometry [J]. *International Journal of Solids & Structures*, 1991, 28(4):471-490.

[8] Erdönmez C. n-tuple complex helical geometry modeling using parametric equations [J]. *Engineering with Computers*, 2013, 30(4):715-726.

[9] Stanova, E. Fedorko, G.; Fabian, M.; Kmet, S. Computer modelling of wire strands and ropes Part I: Theory and computer implementation [J]. *Advances in Engineering Software*, 2011, 42(6): 305-315.

[10] Stanova, E. Fedorko, G.; Fabian, M.; Kmet, S. Computer modelling of wire strands and ropes Part II: Finite element based applications [J]. *Advances in Engineering Software*, 2011, 42(6): 322-331.

[11] Guo Wei, Lu Zhengxiong, Zhang Wu. Geometric modeling theory of bent wire rope based on Pro/E [J]. *China Mechanical Engineering*, 2015, 26(17): 2363-2368